Appl. Phys. A 70, 235–238 (2000) / Digital Object Identifier (DOI) 10.1007/s003390000395

Applied Physics A
Materials
Science & Processing

Rapid communication

Normal-incidence pulsed-laser deposition: better method for fabrication of multilayer structures

I.J. Jeon, D. Kim, J.S. Song, J.H. Her, D.R. Lee, K.-B. Lee

Department of Physics, Pohang University of Science and Technology, 790-784 Pohang, Korea
(Fax: +82-562/279-3099, E-mail: injoon@anyon.postech.ac.kr)

Received: 23 September 1999/Accepted: 5 October 1999/Published online: 21 January 2000 – © Springer-Verlag 2000

Abstract. A new normal-incidence pulsed-laser deposition method is presented. Fe/Mn multilayers were fabricated using both 45°- and normal-incidence deposition of a pulsed laser and were characterized using the small-angle X-ray reflectivity measurement. This new method provides much better control of the lateral uniformity and layer thickness than the 45°-incidence deposition method.

PACS: 81.15.Fg; 61.10.Kw; 68.55.Jk

During the past decades, multilayer (ML) structures have attracted many researchers because they may provide ways to develop new materials. In ML structures, materials with different physical, chemical and/or optical properties are placed next to each other. MLs show exotic behaviors such as giant magneto-resistance (GMR) [1, 2], vertical anisotropy of the magneto-optical effect [3], enhanced normal-incidence reflectivity [4] in soft X-ray regions, and more.

ML structures unavoidably have roughness at their interfaces, which has been known to significantly affect their physical and/or optical properties. Roughness significantly reduces the reflectivity of an ML soft X-ray reflector such as Mo/Si ML [4–6]. On the other hand, the roughness increases the GMR effect in a Fe/Cr ML [7]. In the case of Co/Cu MLs, the roughness decreases or increases the GMR effect, depending on how the current flows [8, 9]. Although it is believed that the spin-dependent scattering at the interface might play an important role in the change in the GMR effect resulting from roughness, further investigations are still needed for a better understanding. This clearly indicates that the ability to fabricate MLs with sharp interfaces and to control the degree of roughness is critical to systematic investigations.

Among various ML fabrication methods, pulsed laser deposition (PLD) has recently become popular owing to the successful fabrication of thin films of oxide materials, such as high-temperature superconducting [10, 11] and ferroelectric materials [12]. The advantages of PLD are (1) that the stoichiometry of a target is maintained in fabricated films, (2) that the deposition under a broad range of ambient pressures of various gases is possible, (3) that the spectrum of materials that can be vaporized is wide and, (4) most importantly, that the system is simple. However, the fabrication of MLs with sharp interfaces by using PLD has not been quite successful. The thickness profile of an ML fabricated by PLD is not uniform because of the high directionality of the plume and the change of the plume's direction during deposition [13]. There have been theoretical and experimental efforts to improve uniformity, such as placing a substrate off-axis, the translation of a substrate, in addition to rotation and laser beam scanning [14–16]. Recently, with a large and complex PLD system, a uniform coating on a 4″-diameter wafer has been achieved [17]. This demonstrates that PLD can also coat a large substrate, but this system is complex and expensive, discouraging its wide-spread use.

1 Normal-incidence pulsed laser deposition

In this paper we describe a new normal-incidence PLD (NIPLD) method which can provide a way to fabricate high-quality MLs by using an inexpensive, small PLD system. Fe/Mn MLs were fabricated by both NIPLD and conventional 45°-incidence PLD (CIPLD). The comparison shows that superior MLs are fabricated by NIPLD when it comes to the lateral uniformity, layer-by-layer thickness control and roughness at an interface. A schematic diagram of a NIPLD system is shown in Fig. 1a. The main difference from a CIPLD system is that a laser beam is incident perpendicularly onto the target surface. This geometry has been used to study particulate production [18] and energy distribution of particles in PLD [19]. However, to our knowledge the fabrication of MLs by using NIPLD and their characterization have not yet been reported.

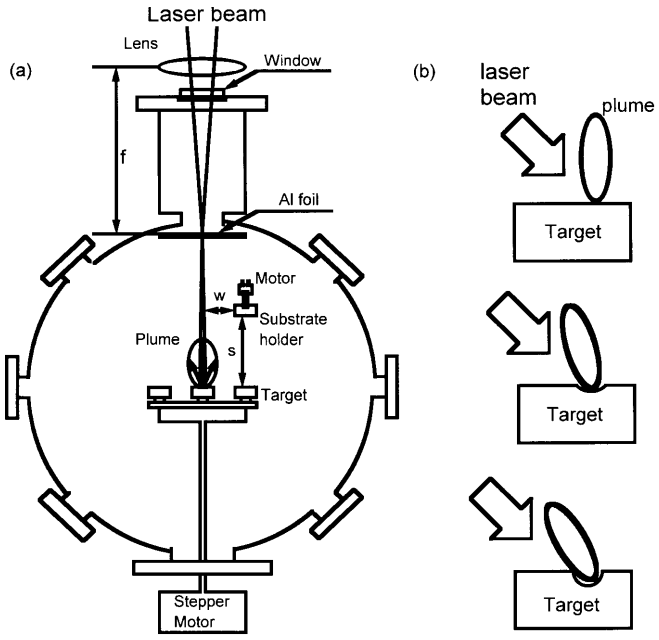

Fig. 1. Schematic diagram of the normal-incidence pulsed laser deposition system

When using a CIPLD system, the change in the plume's direction during deposition, as shown in Fig. 1b, makes it difficult to fabricate high-quality MLs. As the laser beams hit the target, a crater or trench is created. As the crater becomes larger, the normal direction of the surface where the laser beams hit changes and the laser beam absorption becomes non-uniform. These effects lead to a continuous change in the plume's direction. This effect is severe, especially for soft materials (e.g. non-metallic materials).

When we use a CIPLD it is quite difficult to fabricate MLs with more than 15 bilayers that require stringently controlled layer thickness, as for X-ray reflectors. Laser-beam scanning has been introduced to avoid trenching. However, then the off-axis distance (w) changes, leading to a non-uniform coating on the substrate. Consequently, substrate translation, in addition to rotation, has to be implemented. In general, the larger the laser scanning and the translation distance, the better the uniformity. Therefore the system becomes complicated and expensive.

In NIPLD, however, the plume orientation does not change even though trenching occurs. The laser beam is incident normal to the target surface, the surface normal is not significantly changed, and the laser energy is absorbed uniformly so that the plume always exists perpendicular to the surface. The off-axis distance does not change significantly because the surface normal always remains almost constant, and the laser beam is not scanned. It is more desirable to oscillate the target than to scan the laser beam, thereby keeping the off-axis distance fixed. The fluence changes because the trenching changes the morphology of a surface. For soft materials, this effect can change the deposition rate. For hard materials, this effect is negligibly small.

In NIPLD, the window through which the laser beam passes is more easily coated than in CIPLD since the plume always goes directly to the window. This coating reduces the transmission of the window and eventually alters the deposition rate. To block the plume and minimize the coating, a pinhole on an aluminum foil is positioned at the focal position of a focusing lens, as shown in Fig. 1a. The laser is thus slightly defocused on the target surface. The pinhole was drilled by the laser so that the size of the pinhole is just enough for the laser beam to pass through. Nevertheless the window is still coated, although only a little. After a run of deposition, the window is rotated so that a new area may be placed in the laser beam's path.

In order to reduce the production of particulates, the laser fluence on the target should be minimized as much as possible. When the fluence is too small, a thin film deposited on a substrate is laterally non-uniform. In general, uniformity improves as the target-to-substrate distance becomes large. In this case, for a reasonable deposition rate, a large amount of plume is required, which means a large fluence. However a large fluence tends to generate many particulates, which are detrimental to the fabrication of high-quality ML films. On the other hand, the reduction of the fluence results in a smaller amount of plume. In this case, the substrate has to be put closer to the target. Consequently the uniformity becomes worse. For lateral uniformity, the fluence has to be optimized with respect to the target-to-substrate distance.

2 Results and discussion

In this work, Fe/Mn MLs were fabricated on a native oxide Si (100) wafer by using both NIPLD and CIPLD. The base pressure was 8×10^{-7} Torr. The target manipulation system can hold up to four targets. A computer-controlled stepping motor is used to rotate the targets on their axes and to select one target. A direct current motor is attached to a substrate holder to rotate a substrate. The sample–target distance (s) and the off-axis distance (w), in Fig. 1a, were optimized by moving the substrate back and forth and left and right, respectively, until an appropriate uniformity was obtained. The optimized separation (s) was 6 cm. The optimized off-axis distance (w) was 2 cm for CIPLD and 1 cm for NIPLD. The second harmonic of an Nd:YAG pulsed laser (pulse width 5 ns FWHM, 532 nm at a repetition rate of 10 Hz) was used to ablate the target materials. The laser fluence on the target was about $1.8\,\mathrm{J/cm^2}$ for Fe and $0.5\,\mathrm{J/cm^2}$ for Mn. The deposition rate was calibrated by measuring the thickness of test single-layer films with an X-ray diffractometer. The layer thickness was deduced by fitting computer-generated X-ray diffraction (XRD) data to experimental XRD data. The thickness was then divided by the total number of laser pulses used. In CIPLD, the average deposition rates were about 5×10^{-4} nm/shot for Fe and 4.7×10^{-4} nm/shot for Mn; in NIPLD the rates were and 7.9×10^{-4} nm/shot for Fe and 1.2×10^{-3} nm/shot for Mn. Fe/Mn MLs have been deposited on $1'' \times 1''$ Si (100) wafers (substrate). Due to the optimization of the separation (s) and the off-axis distance (w), only the rotation of the substrate was needed for uniform coating over an $1'' \times 1''$ area. Scanning of the laser beam and translation of substrate were not done. The substrates were held at room temperature during deposition. An Mo buffer layer of about 2.5 nm was deposited to smooth the surface roughness on the Si (100) wafer for all the samples.

Small-angle X-ray scattering (SAXS) measurements have been conducted by using synchrotron radiation at the Pohang Light Source (PLS). Three types of SAXS measurements

were made at the X-ray energies of the Mn K edge and the Co K edge: θ-2θ scans for specular reflectivity, offset θ-2θ scans for off-specular reflectivity and a rocking curve scan. Off-specular intensities were subtracted from specular intensities before analysis. The computer code [5, 6] calculates reflectivity by using dynamical X-ray scattering theory in the recursive formalism [20].

Figure 2 shows the data for the CIPLD samples. The number of bilayers is 15. The calculations are represented by solid lines and the measured intensities by the line and open circles. Note that Kiessig fringes are not clearly resolved and the Bragg peaks are not sharp, indicating a gradual change in the thickness of each layer. It has been known that the fluctuation in the thickness of an ML structure is manifested by the smearing of Kiessig fringes and the broadening of Bragg peaks [5, 21]. By fitting computer-generated SAXS data to the experimental data, bilayer thicknesses were deduced. The best fitting yields that the bilayer thicknesses are 2.18, 3.35, 2.4 and 3.5 nm, as seen in Fig. 2a–d, respectively.

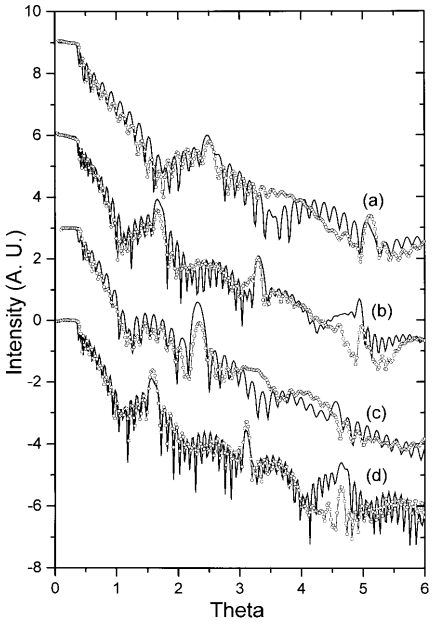

Fig. 2. SAXS data (*line with open circles*) and fitting (*solid line*) for a Fe/Mn ML made by CIPLD

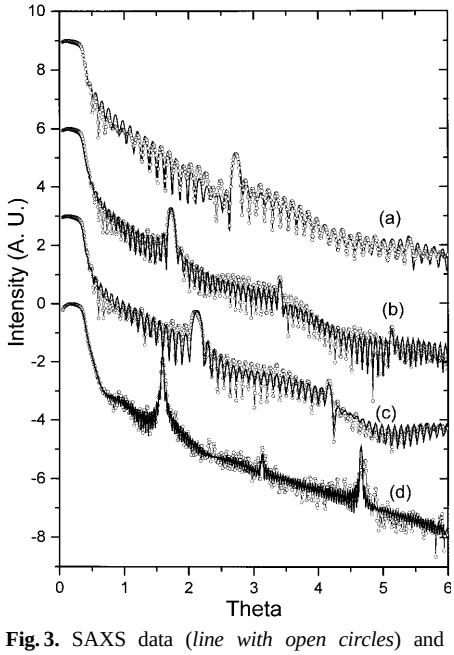

Fig. 3. SAXS data (*line with open circles*) and fitting (*solid line*) for a Fe/Mn ML made by NIPLD

Table 1. Parameters of NIPLD samples deduced from fitting for Fig. 3

	N^*	d /nm	d_{Fe} /nm	d_{Mn} /nm	$\sigma_{\mathrm{Fe/Mn}}$ /nm	$\sigma_{\mathrm{Mn/Fe}}$ /nm	$\varrho^{\dagger}_{\mathrm{Fe}}$	$\varrho^{\dagger}_{\mathrm{Mn}}$
(a)	20	1.71	0.60	1.11	0.38	0.53	2.06	1.67
(b)	20	2.71	1.34	1.37	0.46	0.37	1.82	1.49
(c)	20	2.19	0.60	1.59	0.40	0.51	2.06	1.52
(d)	40	2.98	1.50	1.48	0.29	0.35	2.04	1.66

* number of layers, † number of electrons/$(0.1\ \mathrm{nm})^3$

A series of Fe/Mn MLs with the different bilayer thicknesses were made in NIPLD. The experimental XRD data (line and open circle) are shown in Fig. 3. The number of layers is 20 except for the sample of Fig. 3d, which has 40 layers. The NIPLD samples show sharp Bragg peaks and regular and clear Kiessig fringes, which indicate that the layer thickness is uniform and the interface roughness is small. To investigate the lateral uniformity, XRD measurements were made on five different areas of a sample. The XRD measurements on each area were almost the same, within 1%. Figure 3 shows the excellent fit of the calculations (solid line) to the SAXS data. By fitting [6], the structural parameters such as the bilayer thickness (d), Fe and Mn electron densities (ϱ), and the total interface width (σ) are deduced, as listed in Table 1. The σ contains the contributions both from roughness and from diffusion at interfaces. We have grown ultrathin layers of Fe, ranging from 0.6 nm, corresponding to several monolayers of Fe, to 1.6 nm. The interfaces are very smooth. In the case of Fig. 3d, the 2nd-order Bragg peak is suppressed because the ratio $d_{\mathrm{Fe}}/d_{\mathrm{total}}$ is 0.5. The 3rd-order Bragg peak begins to split. This splitting is caused by the gradual change in deposition rate due to the coating on a vacuum window. This sample is the thickest, the deposition of which took longer than other samples, with enough time for significant coating on the window. If the coating on the window is further minimized, the fabrication of even thicker ML film with the same quality as Fig. 3a, and 3b would be possible.

3 Conclusion

We have demonstrated that NIPLD is capable of fabricating MLs that are superior to those produced by CIPLD. It was shown that a uniform ML with sharp interface and smaller roughness can be fabricated in a simple NIPLD configuration. We anticipate that further prevention of deposition on the vacuum window will allow us to fabricate thicker samples with excellent layer thickness uniformity and small roughness.

Acknowledgements. This work has been supported in part by the Korea Science and Engineering Foundation (Project No. 96-0702-01-01-3) and the Basic Science Research-Institute Program, Korean Ministry of Education (Project No. BSRI-98-2439).

References

1. S.S.P. Parkin, R. Bhadra, K.P. Roche: Phys. Rev. Lett. **66**, 2152 (1991)
2. S.T. Purcell, W. Folkerts, M.T. Johnson, N.W.E. McGee, K. Jager, J. aan de Stegge, W.B. Zeper, W. Hoving: Phys. Rev. Lett. **67**, 903 (1991)
3. F.J.A. Broeder, W. Hoving, P.J.H. Bloemen: J. Magn. Magn. Mater. **93**, 562 (1991)
4. D. Kim, H.W. Lee, J.J. Lee, J.H. Je, M. Sakurai, M. Watanabe: J. Vac. Sci. Technol. A **12**, 148 (1994)
5. D. Kim, D. Cha, S. Lee: J. Vac. Sci. Technol. A **15**, 2291 (1997)
6. D.R. Lee, Y.J. Park, D. Kim, Y.H. Jeong, K.-B. Lee: Phys. Rev. B **57**, 8786 (1998)
7. E.E. Fullerton, D.M. Kelly, J. Guimpel, I.K. Schuller, Y. Bruynseraede: Phys. Rev. Lett. **68**, 859 (1992)
8. A. Howson, M.J. Waker, N. Wiser, D.G. Wright: J. Magn. Magn. Mater. **110**, L239 (1992)
9. M.J. Hall, B.J. Hickey, M.A. Howson, M.J. Walker, J. Xu, D. Greig, N. Wiser: Phys. Rev. B **47**, 12 785 (1993)
10. M. Lorenz, H. Hochmuth, D. Natusch, H. Borner, G. Lippold, K. Kreher, W. Schmitz: Appl. Phys. Lett. **68**, 3332 (1996)
11. W. Prellier, B. Mercey, Ph. Lecoeur, J.F. Hamet, B. Raveau: Appl. Phys. Lett. **71**, 782 (1997)
12. R. Dat, J.K. Lee, O. Auciello, A.I. Kingon: Appl. Phys. Lett. **67**, 572 (1995)
13. T. Venkatesan, X.D. Wu, A. Inam, J.B. Wachtman: Appl. Phys. Lett. **52**, 1193 (1995)
14. D.B. Chrisey, G.K. Huber: *Pulsed Laser Deposition of Thin Film* (Wiley, New York 1994) pp. 293–311
15. J.A. Greer, M.D. Tabat: J. Vac. Sci. Technol. A **13**, 1175 (1995)
16. N. Arnold, D. Bäuerls: Appl. Phys. A **68**, 363 (1999)
17. M. Panzner, R. Dietsch, Th. Holz, H. Mai, S. Vollmar: Appl. Surf. Sci. **96–98**, 643 (1996)
18. R.J. Kennedy: Thin Solid Films 214, 223 (1992)
19. T.N. Hansen, J. Schou, J.G. Lunney: Appl. Phys. Lett. **72**, 1829 (1998)
20. J.H. Underwood, T.W. Barbee Jr.: Appl. Opt. **20**, 3027 (1981)
21. D. Kim, D. Cha: J. Kor. Phys. Soc. **29**, 74 (1996)